Defense Technical Information Center Compilation Part Notice

ADP012175

TITLE: Molecular Engineered Porous Nanocomposites of Metal Oxide and Clay Using Surfactants

DISTRIBUTION: Approved for public release, distribution unlimited

This paper is part of the following report:

TITLE: Nanophase and Nanocomposite Materials IV held in Boston, Massachusetts on November 26-29, 2001

To order the complete compilation report, use: ADA401575

The following component part numbers comprise the compilation report:
ADP012174 thru ADP012259

Mat. Res. Soc. Symp. Proc. Vol. 703 © 2002 Materials Research Society V1.5

Molecular Engineered Porous Nanocomposites of Metal Oxide and Clay Using Surfactants

Huai Y. Zhu and Gao. Q. Lu*
NanoMaterials Centre and Department of Chemical Engineering, The University of Queensland
St Lucia Qld 4072 Australia

ABSTRACT

A novel synthesis route of metal oxide nanoparticles dispersed in a silicate framework is reported here. This composite nanostructure is highly thermally stable and porous, rendering large surface area and rich surface chemistry promising for catalytic applications. Aqueous solutions of metal salts were used as the precursors of the nanoparticles, and added in an aqueous dispersion of synthetic clay, laponite, in which the clay exists in exfoliated silicate sheets. Acid leaching of the clay sheets occurs in the reaction due to the strong acidity of the metal salt solution. Meanwhile, the metal hydrate ions polymerise because of the high pH of the clay dispersion and condense on the leached silicates. This mechanism is distinctly different from conventional pillaring process. The nanocomposites of various oxides and binary oxides were synthesised. By introducing polyethylene oxide surfactants, we obtained mesoporous nanocomposites with very large surface areas (400 –900 m^2/g) and porosity. These nanocomposites are superior catalysts or catalyst supports over of microporous pillared clays [1-3] due to their structure and surface properties.

INTRODUCTION

The nanoparticles of transition metal oxides, in several nanometers range, are very attractive materials for uses in catalysis, because these nanoparticles often exhibit superior properties and performance due to their large specific surface area. However, agglomeration of ultra-fine particles adversely affects their performance, and recovering such catalysts is difficult. These problems seriously limit their applications. A feasible approach is to disperse nanoparticles of metal oxide within an inorganic media, such as layered clays, meanwhile maintaining most of the surface of metal oxides accessible to reactant molecules. This approach is similar, in some aspects, to the synthesis of pillared layered clays developed in late 1970s [1-2].

It is well known that hydrate cations of many metal elements exist stably in acidic environment. If the pH increases, the metal hydrate ions hydrolyze, forming polymerized hydroxyl ions (oligomers), and finally precipitates [4]. Actually, there are layered clays, which can form well-dispersed suspensions at high pH values. For instance, laponite, synthetic clay that is iso-structural with the smectite clays, has a pH between 9.5 and 10. This pH is effective for inducing hydrolysis of various metal ions. The clay platelets are small, about 20-30 nm in diameter. In a dilute aqueous dispersion the clay exists as discrete plates [5]. Therefore, laponite is an ideal inorganic medium to form nanometer-scale composite structures with various metal hydroxyl species. Aqueous solutions of metal hydroxyl species or positively charged sol particles (precursor solutions) can be readily obtained from inorganic salts. The development of pillared layered clays has provided very useful knowledge on the precursor solutions [1]. The structures

of various oligomers in precursor solutions have been comprehensively studied [6,7]. In many cases, the pillaring solutions for the synthesis of pillared layered clays can be used for the synthesis of nanocomposites.

EXPERIMENTAL DETAILS

A general procedure for synthesis of metal oxide nanoparticles in clays is as follows: Laponite clay was dispersed into water in a designed ratio to form a clear dispersion. A certain amount of a polyethylene oxide (PEO) surfactants of small molecular weights, with a general chemical formula $C_{12\text{-}14}H_{25\text{-}29}O(CH_2CH_2O)_nH$ (n = 5-12), was added into the laponite dispersion which then became opaque. The suspension was stirred for 2 hours to allow sufficient mixing. To this mixture, an aqueous solution of metal ions was added drop-wise with continuous stirring. Some solutions of metal ions were obtained following the method for preparing corresponding pillaring solutions. The pH was controlled at 3-5. For instance a solution containing zirconium hydroxyl oligomers can be readily prepared by reflux a $ZrOCl_2$ solution. After a stirring of 2 hour, the mixed suspension was maintained at 373K for two days. The precipitate was recovered from the mixture by centrifuging and washed with deionized water. The wet cake was dried in air and calcined at 773 K for 20 hours. The hydrolyzed metal hydroxyl species are converted to oxide particles of several nanometers, and porous nanocomposite structures of metal oxide and silicate are obtained.

RESULTS AND DISCUSSION

We found that the porosity of the nanocomposite can be significantly increased by introducing polyethylene oxide (PEO) surfactants of small molecular weights. These surfactants have strong affinities to the surfaces of clay and metal hydrates. Therefore, they have a function of separating the hydrolyzed species of metal elements, preventing them from further agglomeration and sintering during the drying and heating processes. It is known that in the templated synthesis the pore size of the product is proportional to the molecular size of the surfactant [8-10]. But there is no such a trend observed in this study. The molecular size of the surfactant is not a sole determinant of the pore size of the product solids. During heating the surfactant volatilizes, leaving a rigid structure with high porosity. The BET specific surface area and porosity data of some nanocomposite samples are given in Table 1.

These oxide nanocomposites exhibit much larger surface areas and pore volumes, compared to pillared layered clays (pore volume of 0.15-0.40 cm^3/g and the BET surface area 150-400 m^2/g). The pillared layered clays are microporous solids (pore size below 2 nm) with a moderate porosity, while the nanocomposites are mesoporous solids. The structures of these two classes of solids are also profoundly different. The TEM images of the pristine laponite and three nanocomposites (as representatives) are given in Fig 1.

Table I. BET specific surface area and pore volume of metal oxide nanocomposite samples.

Samples prepared w/surfactant			**Samples prepared w/o surfactant**		
Metal oxide	BET S.A. (m^2/g)	Vp (cm^3/g)	Metal oxide	BET S.A. (m^2/g)	Vp (cm^3/g)
Al_2O_3-	542	0.709	Al_2O_3-	278	0.233
Al_2O_3/La_2O_3-	587	0.676	Al_2O_3/La_2O_3-	439	0.383
Al_2O_3/CeO_2-	599	0.775	Al_2O_3/CeO_2-	422	0.345
ZrO_2	459	0.430	ZrO_2	248	0.146
ZrO_2/CeO_2	611	0.676	ZrO_2/CeO_2	291	0.185
TiO_2-	635	0.776	TiO_2-	343	0. 405
Cr_2O_3-	670	0.461	Cr_2O_3-	894	1.124
Fe_2O_3-	434	0.547	Fe_2O_3-	419	0.307

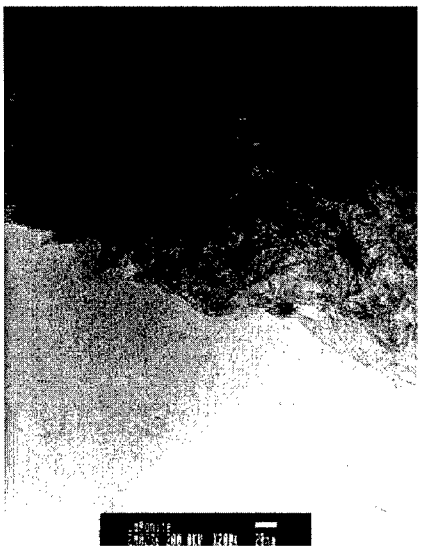

(a)

(b)

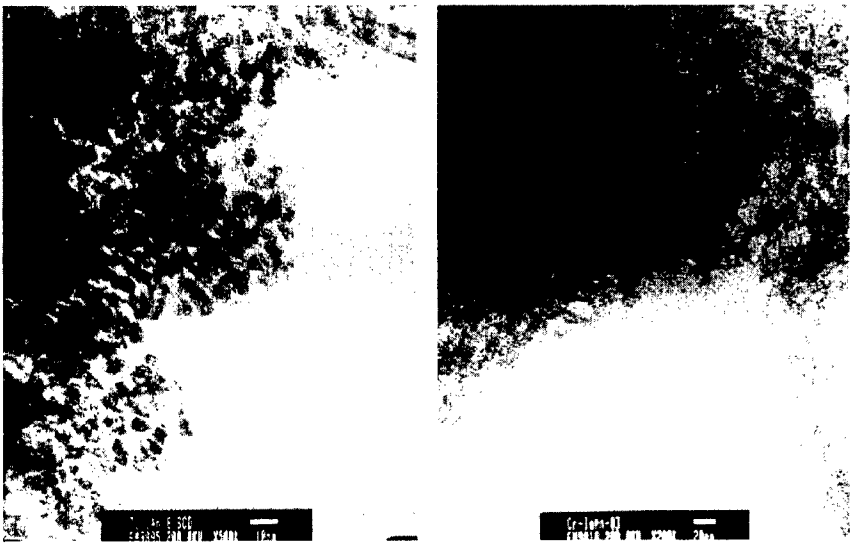

(c) (d)

Figure 1. TEM images of laponite clay and the calcined metal oxide nanocomposite samples. **(a)** laponite (**b**) Al_2O_3-nanocomposite (**c**). TiO_2-nanocomposite and (**d**) a Cr_2O_3-nanocomposite with low Cr_2O_3 content. The scale bars in the images indicate 20 nm.

Bundles of several clay platelets can be seen in the image of pristine laponite in Fig 1a, which aggregate in a poor long-range order. For pillared clays, the clay layers were regarded as inert with respect to reaction and almost intact in term of chemical composition during the pillaring process. However, layered clays can react with various acids even at moderate conditions [11-13]. Acid leaching is regarded as an effective means to activate clays. The acid leaching could result in remarkable changes in composition and structure of the clay layers. The extent of the reaction varies substantially from clay to clay.

Fig 1b is the image of the sample prepared from a solution containing Keggin ions [1,2,7] $[Al_{13}O_4(OH)_{24}]^{7-}$, and the laponite dispersion, Al_2O_3-composite. In this solid, thin stringy structure of about 1 and 2 nm thickness are observed, which are singular and paired silicate platelets, respectively. It is noted that these platelets are entangled but with a separation in the nanometer range. This indicates that the platelets are intercalated with nanoparticles of alumina. The Keggin ion solution has a weak acidity (pH of 3.0-3.5), and there is no obvious acid leaching from the laponite platelets, according to the results of chemical composition of the sample (in Table 2). Substantial loss of magnesium that is in the clay layer is an indicative of the acid leaching. Thus, the laponite platelets remain intact, in terms of composition and framework structure. When a more acidic solution containing sol particles of titanium (IV) hydrate, was used, laponite platelets are obviously involved in reaction. Most of magnesium in the clay platelets was leached out (Table 2). The solids obtained after calcination at 500°C contains mainly silica and titanium dioxide. X-ray powder diffraction pattern (not shown) indicates that

TiO_2 exists in anatase phase and we can see the aggregation of crystallites with random orientations in Fig 1c. The size of the anatase crystallites can be estimated from domains of regular texture in the image, being about 3-9 nm. Neither the x-ray pattern nor TEM image indicate any crystal form of silica or silicate although silica accounts for over 50% of the sample mass. The silica in the samples is more likely amorphous as reaction product of the laponite clay. Similar behaviors were observed for other transition metal oxide nanocomposites. Energy dispersing x-ray spectroscopy (EDS) was used to analyze the chemical compositions at different regions over a sample. At least 5 regions were taken for one sample and the average region size was about 15 nm in diameter. We found no obvious difference from region to region and the overall composition of the sample was uniform, for all samples. This means that in these samples metal oxide particles homogeneously disperse in exfoliated silicate media.

Table II. Major chemical composition of the samples shown in Fig 1.

Sample	SiO_2 (%)	Al_2O_3 (%)	MgO (%)	TiO_2 (%)	Na_2O (%)	Fe_2O_3 (%)	Cr_2O_3 (%)
Laponite	51.10	0.07	23.20	-*	2.51	-	-
Al_2O_3-composite	41.49	27.91	17.38	-	-	0.04	-
TiO_2-composite	55.30	0.12	0.19	43.90	-	0.02	-
Cr_2O_3-composite	79.87	-	6.13	-	-	0.60	0.03

* Not detectable.

The image in Fig 1d provides more information on the structure of the reaction product derived from laponite. This solid was obtained after reaction of laponite suspension with a solution containing chromium hydroxyl ions. In this particular case, only a small amount of Cr_2O_3 is left in the product solid (Cr_2O_3 content below 1 %), which contains about 80 wt% of silica and 6 wt% of MgO, meanwhile most of the Mg content in the original laponite has been leached out during the synthesis. This solid provides a clear picture of the residue from the original laponite after reaction. The structure of this solid is strikingly different from that of the original laponite. Mesopores ranging from 3-20 nm can be seen in the image. These irregular pores reveal that the laponite platelets were seriously attacked, not only at edges but also on the basal surface of the platelets (gallery access mechanism [13], leaving a porous framework of silica.

^{29}Si magic angle spinning nuclear magnetic resonance (^{29}Si MAS-NMR) of the samples (Fig 2) also indicates the different structure change in silicate platelets caused by the reaction. ^{29}Si MASNMR spectrum of laponite displays two resonance peaks at –90 and 80 ppm. Such chemical shifts are correlated to the SiO_4 tetrahedra linked with 3 and 2 other SiO_4 tetrahedra (Q^3 and Q^2 sites), respectively. This is expected for the structure of laponite clay layer [14-15]. In the clay layer most SiO_4 tetrahedra are linked to 3 other SiO_4 tetrahedra, being in Q^3 sites but the tetrahedra at the edges of the clay layers are linked to 2 other SiO_4 tetrahedra and thus form the Q^2 sites. The smaller amount of Q^2 sites, compared with that of Q^3 sites, is responsible for the low intensity of the peak at -80 ppm.

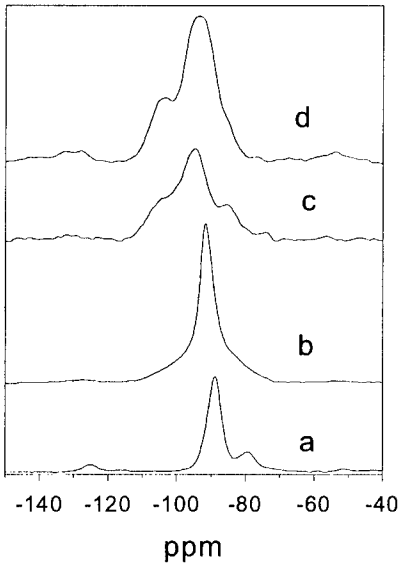

Figure 2. ^{29}Si magic angle spinning nuclear magnetic resonance (^{29}Si MASNMR) of **a.** laponite clay; **b**, Al_2O_3-nanocomposite; **c**, TiO_2-nanocomposite; and **d**, Cr_2O_3-nanocomposite with low Cr_2O_3 content.

The chemical shifts for Al_2O_3-nanocomposite is similar to that of laponite, with a major resonance at –91.7 ppm. This means that the clay platelets remain almost intact during the reaction, being consistent with our observation in TEM image. The TiO_2-nanocomposite and Cr_2O_3- nanocomposite samples show substantially different MAS-NMR spectra. Broad resonance in the range from –110 to –80 ppm can be seen, reflecting poor short-range order. It also suggests a radical structure change of the silicate due to the reaction in the synthesis. The chemical shift at –104 ppm (a peak for Cr_2O_3-nanocomposite and a shoulder for TiO_2-nanocomposite) should be assigned to Q^4 sites where the SiO_4 tetrahedra linked with 4 other SiO_4 tetrahedra. In laponite clay structure there should be no Q^4 sites [16] and this is confirmed by the spectrum of the clay. Thus the Q^4 sites must have resulted from the profound structure changes of the silicate in the synthesis.

This evidence suggests that the clay layers could be seriously attacked if the acidity of the precursor solution is strong. On the other hand, the laponite dispersion with a high pH inevitably induces further hydrolysis of the metal hydroxyl oligomers in the precursor solution, forming larger species, the precursors of metal oxide nanoparticles. These large species most likely condense to the surrounding silicate platelets, because they carry opposite electric charges. This leads to a composite structure in which metal oxide particles of several nanometers in size are dispersed among the exfoliated silicate media.

According to this mechanism, it is possible to alter the particle size of the metal oxides by manipulating the acidity of the precursor solution. Indeed, as we increased the H^+/Ti molar ratio of the precursor solution from 2.0 to 8.0, the mean size of anatase particle in the product TiO_2-composites increases from 3.7 to 9.0 nm. This finding is of importance, which allows us to effectively tailor the structure of these solids for various applications.

During last two decades, application of pillared clays as catalysts or catalyst supports for numerous chemical reactions has been attempted [3]. In general, better acidic characteristic, larger specific surface area, pore volume and pore size are required for catalysis purpose. As shown above, the properties of nanocomposites based on the above properties are remarkably superior to that of pillared clays and they are of great potential for these catalytic applications.

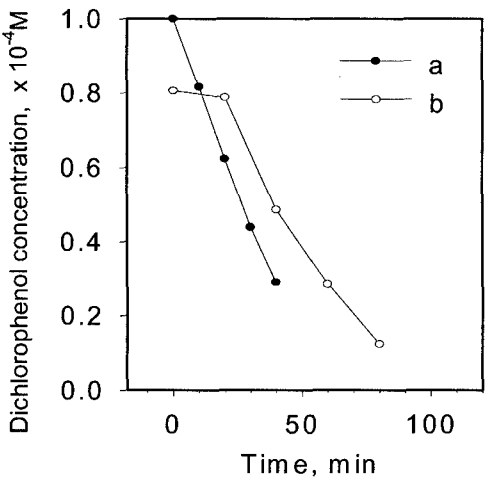

Figure 3. Catalytic performance of photocatalysts for photo-degradation of 2, 4-dichlorophenol. Curves **a** and **b** illustrate the performance of the ultra-fine TiO_2 powder P25 and a TiO_2-nanocomposite sample, respectively.

TiO_2-nanocomposite prepared in this study can be used as photocatalysts. It is well known that TiO_2 anatase nanoparticles are regarded as the best photo-catalysts for decomposing refractory organic pollutants in water and air [17-19]. The catalyst can be used for various processes such as odor elimination of drinking water, degradation of harmful organic contaminants, like herbicides, pesticides, refractive dyes, and oil spills in surface water systems. In Fig 3 catalytic performances for photo-degradation of 2, 4-dicholorophenol by a TiO_2-composite and P25, a commercial ultra-fine titanium dioxide powder supplied by Degussa, are compared. The overall photo-catalytic efficiency of the TiO_2-nanocomposite is comparable to that of P25, which is known to be the best commercial TiO_2 photo-catalyst and has a mean particles size of about 25 nm. The performance of the TiO_2-nanocomposite proves that most of the surface of TiO_2 crystals is accessible to the various molecules in solution. Furthermore, the TiO_2-nanocomposite contains about 45 % of TiO_2. Therefore, the activity per mass of TiO_2 for the TiO_2-nanocomposite is superior. Besides, it is very difficult to recover P25 powder from

water. This could leads to a potential difficulty in downstream separation. In contrast, the nanocomposite catalyst can be readily separated from aqueous solutions by settling and filtration. The silicate layers in the samples not only act as media allowing TiO_2 to disperse in nano-crystals but also link the distributed TiO_2 nano-crystals to large granules which can be recovered easily.

Besides, we also found that nickel catalysts supported on ZrO_2-nanocomposite result in high conversion rate for methane reforming with carbon dioxide. The catalyst maintains the high activity for over 180 hours (Fig 4), much longer than the catalyst supported activated Al_2O_3. The pore structure and surface nature of ZrO_2-nanocomposite can be tailored to obtain supports with higher surface area resulting in well-dispersed Ni catalysts. Carbon deposition on such catalysts was also suppressed due to the small nanoparticles of Ni metal well dispersed in the nanoporous support. The sintering deactivation is also reduced due to the excellent dispersion.

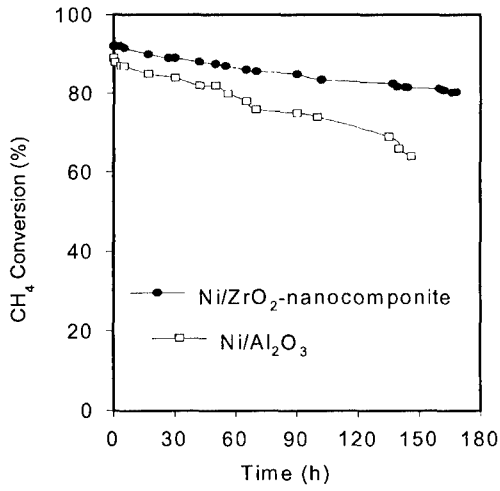

Figure 4. Performance of the nickel catalysts on a ZrO_2-nanocomposite and an activated alumina for methane reforming with carbon in a fixed bed reactor. The reaction conditions CH_4/CO_2 =1:1, P = 1 atm and flow rate = 60 ml/min.

We also found very recently that Fe_2O_3-composite is an excellent catalyst for the photo-assisted Fenton degradation of azo-dye Orange II (Fig 5). This catalyst can significantly enhance the degradation of Orange II and has an excellent long-term stability. It is much cheaper than the Nafion-based catalysts used in Fenton reaction for water purification. It was also found that H_2O_2 molar concentration in solution, solution pH, UV light wavelength and power, and catalyst loading are the four main factors that can significantly influence the photo-assisted Fenton degradation of Orange II.

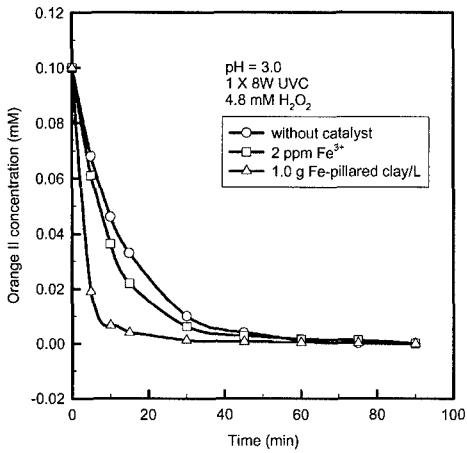

Figure 5. Orange II concentration as a function of irradiation time for systems without any catalyst, with 2 ppm Fe^{3+} in solution, and with 1.0 g Fe-nanocomposite catalyst/L, respectively. The Orange II degradation is much faster in the presence of the Fe-nanocomposite catalyst than that without any catalyst.

CONCLUSIONS

These findings in this work highlight the great potential of this novel synthesis of metal oxide nanocomposites as advanced catalytic materials. These solids can be readily granulated to designed shapes and the grains have good mechanical strength because of the presence of a silicate framework structure. Creating porous structures of transition metal oxides with large surface areas has attracted great research interest. Templated synthesis, invented in early 1990s for the synthesis of mesoporous silica or aluminosilicate [8,9] were also applied for this purpose. Successes have been achieved as various approaches, such as starting with metal alkoxides and conducting the synthesis in non-aqueous systems, were employed to overcome serious difficulties in the synthesis [20-22]. In comparison, the synthesis proposed in this study has a prominent advantage that it can be conducted in aqueous system at moderate conditions. Moreover, this synthesis utilises the reaction between the clay suspension and the oligomer solution to form composite nanostructure with assistance of PEO surfactant, being profoundly different from the synthesis of the well-known pillared clay materials. Actually, such a synthesis route is not limited to laponite, we have also prepared nanocomposites from natural layered clays such as saponite and hectorite. This new synthesis technique allows us to design and engineer composite nanostructures with desirable pore and surface properties.

ACKNOWLEDGEMENTS

Financial Support from the Australian Research Council (ARC) and the University of Queensland are gratefully acknowledged. HYZ is indebted to Australian Research Council (ARC) for the QE II fellowship. The authors would like to thank Dr John Barry for his assistance in TEM imaging, and Dr Andrew Whittaker and Indriana Kartini for their assistance in NMR analysis. We also would like to thank Dr J-C. Zhao for providing data on photocatalytic degradation of dichlorophenol and Dr X. Hu for data on the Fenton reactions for Orange II removal.

REFERENCES

1. R. Burch (Ed.), "*Pillared Clays*", *Catal Today*, Vol 2-3, (Elsevier, New York, 1988).
2. T.J. Pinnavaia, *Science*, **220**, 365-71 (1983).
3. A. Gil., L.M. Gandia, and M.A.Vicente, *Catal. Rev.* **42**(1/2) 145-212 (2000).
4. C.F. Baes and R.E. Mesmer, *The Hydrolysis of Cations*, (Wiley & Sons, New York, 1986).
5. D.W. Thompson and J.T. Butterworth, *J. Colloid Interface Sci.* **151**, 236-243 (1992).
6. K. Ohtsuka, Y. Hayashi and M. Suda, *Chem. Mater.* **5**, 1823-1829(1993).
7. R.A. Schoonheydt, H. Leeman, A. Scorpion, I. Lenotte and P. Grobet, *Clays Clay Miner.* **42**, 518-525(1994).
8. C.T. Kresge, M.E. Leonowicz, W.J. Roth, J.C. Vartuli and J.S. Beck, *Nature*, **359**, 710-712(1992)
9. S. Inagaki, Y. Fukushima, and K. Kuroda, *J. Chem. Soc. Chem. Commun.* 680-682. (1993).
10. Q. Huo, *et al*, *Nature*, **368**, 317-321(1994).
11. A. Corma, A. Mifsud, and E. Sanz, *Clay Miner.* **22**, 225-232(1987).
12. R. Mokaya and W. Jones, *J. Catal.* **153**, 76-85(1995).
13. H. Kaviratna and T.J. Pinnavaia, *Clays Clay Miner.* **42**, 717-723(1994).
14. M.A. Wilson, *NMR Techniques and Applications in Geochemistry and Soil Chemistry*. (Pergamon Press, Oxford, 1987)
15. S. Komarneni, C.A. Fyfe, G.J. Kennedy and H. Strobl, H. *J. Am. Ceram. Soc.* **69**, C45-C47 (1986).
16. A.C.D. Newman, *Chemistry of Clays and Clay Minerals*, (Mineralogical Society, Longman Sci & Tech., UK, 1987) p161.
17. G. Liu, X. Li, J. Zhao, H. Hidaka, and N. Serpone, *Environ. Sci. Technol.* **34**, 3982-3990(2000).
18. A. Fujishima, K. Hashimoto and T. Watanabe, *TiO_2 Photocatalysis Fundamentals and Applications*, (BKC, Inc., Tokyo, 1999) pp50-89.
19. A. L. Linsebigler, G.Q. Lu, and J.T. Yates, *Chem. Rev.* **95**, 735-758(1995).
20. D.M. Antonelli and J.Y. Ying, *Angew. Chem., Int. Ed. Engl.* **34**, 2014-2017(1995).
21. P. Yang, D.Y. Zhao, D.I. Margolese, B.F. Chmelka and G.D. Stucky, *Nature* **396**, 152-155(1998).
22. J.Y. Ying, C.P. Mehnert and M.S. Wong, Synthesis and applications of supramolecular-templated mesoporous materials. *Angew. Chem., Int. Ed,* **38**, 56-77 (1999).